Atomic Layer Deposition of Hafnium Dioxide Films from 1-Methoxy-2-methyl-2-propanolate Complex of Hafnium

Kaupo Kukli,*,† Mikko Ritala,† Markku Leskelä,† Timo Sajavaara,‡ Juhani Keinonen,‡ Anthony C. Jones,§,|| and John L. Roberts§

Department of Chemistry, University of Helsinki, P.O. Box 55, FIN-00014 University of Helsinki, Finland, Accelerator Laboratory, University of Helsinki, P.O. Box 43, FIN-00014 University of Helsinki, Finland, Department of Chemistry and Surface Science Research Centre, University of Liverpool, Liverpool L69 3BX, UK, and Inorgtech Ltd., 25 James Carter Road, Mildenhall, Suffolk, IP28 7DE, UK

Received October 4, 2002. Revised Manuscript Received February 17, 2003

HfO_2 films were grown by atomic layer deposition from a mononuclear and volatile complex $Hf(OCMe_2CH_2OMe)_4$ in the temperature range of 275−425 °C on borosilicate glass and Si-(100) substrates. HfO_2 films were formed as a result of alternate adsorption and hydrolysis steps of the hafnium precursor. The adsorption of hafnium complex was not entirely self-limiting, probably because of the thermal decomposition of the precursors. Crystalline films containing the monoclinic HfO_2 phase were grown at temperatures exceeding 300−325 °C. The refractive index of the films varied between 1.8 and 2.0. The effective permittivities of the dielectrics in Al/HfO_2/Si structures varied between 12 and 17.

1. Introduction

High-permittivity HfO_2 and ZrO_2 based oxides are currently being investigated as replacement materials for SiO_2 and SiON based gate oxides in complementary metal-oxide-semiconductor (CMOS) devices. Both ZrO_2 and HfO_2 are compounds of high chemical stability and may form relatively stable and sharp interfaces with silicon substrate. However, HfO_2 has quite often been preferred because its chemical stability may exceed that of ZrO_2.[1,2]

Several precursors, such as hafnium β-diketonates,[3,4] nitrates,[5] alkoxides,[6] and alkylamides[7,8] have been exploited in chemical vapor deposition or atomic layer deposition of HfO_2 thin films. Halide chemical vapor deposition (CVD) generally requires relatively high substrate temperatures,[9] but $HfCl_4$ and HfI_4 have been used successfully in low-temperature atomic layer deposition (ALD) processes.[10−13] However, the quality of HfO_2 capacitors grown via sublimation of solid halides may sometimes suffer from the particle transport from the solid hafnium precursor,[14] and the possibility of halide contamination is a serious concern in microelectronics applications. It is therefore important to explore alternative precursors.

Hafnium or zirconium β-diketonates do not react with water, but require O_3 as an oxidant in ALD processes,[15] making them unsuitable for gate dielectric applications as the use of ozone causes extensive oxidation of silicon.[16] Metal alkoxides are reactive toward water and have been widely used in MOCVD[17] and ALD.[18] They potentially offer significant process advantages over other precursors. However, the majority of $[Hf(OR)_4]$ complexes are oligomeric with limited volatility, due to the pronounced tendency of the Hf(IV) atom to expand its coordination sphere to six, seven, or eight.[19] To inhibit oligomerization, bulky, sterically demanding

* To whom correspondence should be addressed at Institute of Experimental Physics and Technology, University of Tartu, Tähe 4, EE-51010 Tartu, Estonia. E-mail: kaupok@ut.ee.
† Department of Chemistry, University of Helsinki.
‡ Accelerator Laboratory, University of Helsinki.
§ University of Liverpool.
|| Inorgtech Ltd.

(1) Sneh, O.; Clark-Phelps, R. B.; Londergan, A. R.; Winkler, J.; Seidel, T. E.; *Thin Solid Films* **2002**, *402*, 248.
(2) Gutowski, M.; Jaffe, J. E.; Liu, C.-L.; Stoker, M.; Hedge, R. I.; Rai, R. S.; Tobin, P. J.; *Appl. Phys. Lett.* **2002**, *80*, 1897.
(3) Balog, M.; Schrieber, M.; Patai, S.; Michman, M. *J. Cryst. Growth* **1972**, *17*, 298. Balog, M.; Schrieber, M.; Michman, M.; Patai, S. *Thin Solid Films* **1977**, *41*, 247.
(4) Smith, R. C.; Ma, T.; Hoilien, N.; Tsung, L. Y.; Bevan, M. J.; Colombo, L.; Roberts, J.; Campbell, S. A.; Gladfelter, W. L. *Adv. Mater. Opt. Electr.* **2000**, *10*, 105.
(5) Conley, J. F., Jr.; Ono, Y.; Zhuang, W.; Tweet, D. J.; Gao, W.; Mohammed, S. K.; Solanki, R. *Electrochem. Solid State Lett.* **2002**, *5*, C57.
(6) Choi, K.-J.; Shin, W.-C.; Yoon, S.-G. *J. Electrochem. Soc.* **2002**, *149*, F18.
(7) Gordon, R. G.; Becker, J.; Hausmann, D.; Suh, S. *Chem. Mater.* **2001**, *13*, 2463. Gordon, R. G. *Electrochem. Soc. Proc.* **2000**, *2000−13*, 248.
(8) Kukli, K.; Ritala, M.; Sajavaara, T.; Keinonen, J.; Leskelä, M. *Chem. Vap. Deposition* **2002**, *8*, 199.
(9) Cho, M.-H.; Roh, Y. S.; Whang, C. N.; Yeong, K.; Nahm, S. W.; Ko, D.-H.; Lee, J. H.; Lee, N. I.; Fujihara, K. *Appl. Phys. Lett.* **2002**, *81*, 472.
(10) Ritala, M.; Leskelä, M.; Niinistö, L.; Prohaska, T.; Friedbacher, G.; Grasserbauer, M. *Thin Solid Films* **1994**, *250*, 72.
(11) Aarik, J.; Aidla, A.; Kiisler, A.-A.; Uustare, T.; Sammelselg, V. *Thin Solid Films* **1999**, *340*, 110.
(12) Forsgren, K.; Hårsta, A.; Aarik, J.; Aidla, A.; Westlinder, J.; Olsson, J. *J. Electrochem. Soc.* **2002**, *149*, F139.
(13) Cho, M.; Park, J.; Park, H. B.; Hwang, C. S.; Jeong, J.; Hyun, K. S. *Appl. Phys. Lett.* **2002**, *81*, 334.
(14) Kanniainen, T.; Kattelus, H.; Skarp, J. *Electrochem. Soc. Proc.* **1997**, *1997−31*, 36.
(15) Putkonen, M.; Niinistö, L. *J. Mater. Chem.* **2001**, *11*, 3141.
(16) Gusev, P.; Cartier, E.; Buchanan, D. A.; Gribelyuk, M.; Copel, M.; Okorn-Schmidt, H.; D'Emic, C. *Microelectron. Eng.* **2001**, *59*, 341.
(17) Jones, A. C. *J. Mater. Chem.* **2002**, *12*, 2576.
(18) Ritala, M.; Leskelä, M. In *Handbook of Thin Film Materials*; Nalwa, H. S., Ed.; Academic Press: New York, 2002; Vol. 1 and references therein.

10.1021/cm021328p CCC: $25.00 © 2003 American Chemical Society
Published on Web 04/15/2003

ligands such as *tert*-butoxide have been employed, resulting in the volatile mononuclear complex [Hf(O^tBu)$_4$].[19] However, [Hf(O^tBu)$_4$] contains an unsaturated four-coordinate metal center, and the *tert*-butoxide ligand undergoes a catalytic hydrolytic decomposition reaction in the presence of trace water.[20] These complexes are therefore extremely air- and moisture-sensitive, which limits their shelf life and makes them difficult to handle and use in ALD. Metal *tert*-butoxide complexes, such as [Zr(O^tBu)$_4$], also fail to give self-limiting adsorption in ALD,[21] so we have focused attention on alternative alkoxide ligands which may produce more stable complexes with more favorable ALD behavior.

An established strategy for inhibiting oligomerization in metal alkoxides, as well as increasing the coordination number of the highly positively charged central metal atoms, is to incorporate bidentate donor-functionalized alkoxide ligands into the complex.[22] It has been shown recently that the donor-functionalized ligand 1-methoxy-2-methyl-2-propanolate ($OCMe_2CH_2OMe$, mmp) can be used to inhibit the oligomerization of Zr and Hf alkoxides, and the syntheses and structural characterization of the volatile mononuclear complexes [Hf(O^tBu)$_2$(mmp)$_2$] and [Hf(mmp)$_4$] have recently been reported.[23] Both precursors have been used successfully for the deposition of HfO_2 by liquid injection CVD in the temperature range 350−650 °C using O_2 as oxidant.[24] The HfO_2 films were subsequently shown to have good dielectrical characteristics,[25] and this has encouraged us to investigate the application of these compounds for the ALD of gate dielectric oxides.

In the present study, HfO_2 films were atomic-layer-deposited from a novel liquid hafnium precursor, hafnium tetrakis(1-methoxy-2-methyl-2-propanolate), Hf($OCMe_2CH_2OMe$)$_4$, and H_2O in order to investigate the basic features of the film growth with this new precursor combination, as well as the dielectric behavior of the resulting films.

2. Experimental Section

The films were grown in a hot-wall horizontal flow-type ALD reactor[26] mainly onto borosilicate glass substrates. Some samples were grown on p-Si(100) at 360 °C. The p-Si(100) substrates were covered with 1.2−1.8 nm thick chemical SiO_2. At 300, 325, and 425 °C, the films were deposited on n-Si(100) substrates which were, prior to deposition, etched in hydrofluoric acid (1% aqueous solution) for 25 s to remove the native oxide and then rinsed with deionized water. The substrate temperature was varied in the range of 275−425 °C. The pressure in the reactor was about 10 mbar. Hf(mmp)$_4$ was evaporated from an open boat at 70−100 °C, respectively, inside the reactor. H_2O vapor was generated in an external reservoir at room temperature and led into the reactor through needle and solenoid valves. Metal precursor pulse length was varied between 0.2 and 1.8 s, while the water pulse length was in the range of 0.5−1.0 s. Constant purge times of 0.5 s were used after each precursor pulse to separate the precursor flows in the gas phase and to remove the excess reactants and gaseous reaction byproducts from the reactor. The number of growth cycles applied varied between 780 and 2500. Nitrogen was used as both precursor-carrier and purge gas.

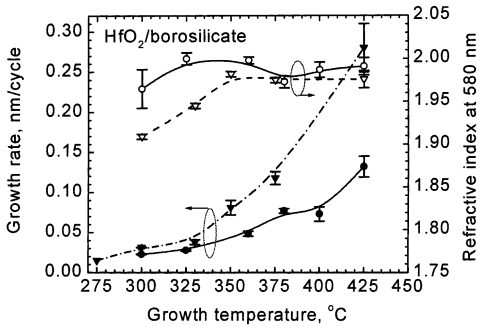

Figure 1. Growth rate and refractive index of HfO_2 films deposited from Hf(mmp)$_4$ and H_2O as functions of growth temperature. The Hf precursor pulse lengths were 0.4 s (circles) and 1.0 s (triangles). The H_2O pulse and purge times were 0.5 s. The error bars express the variation of the refractive index and film thickness in each sample along the substrate length of 4 cm. Lines are guides to the eye.

Film thickness and optical properties were calculated from optical transmission spectra[27] measured by a Hitachi U-2000 spectrophotometer. Structure of the films films was determined by means of a Philips MPD 1880 powder X-ray diffractometer (XRD) using Cu Kα radiation and the Bragg−Brentano geometry. The film composition and residual contamination levels were evaluated by time-of-flight elastic recoil detection analysis (TOF-ERDA).[28] A 53-MeV $^{127}I^{10+}$ beam for TOF-ERDA was obtained from a 5-MV tandem accelerator EGP-10-II, and forward-scattered iodine ions and recoiled target atoms were used for the determination of Hf and lighter elements, respectively.

Dielectric properties were measured after e-beam evaporation of aluminum through a shadow mask, depositing dot electrodes with the effective area of 0.204 mm^2 on the top of HfO_2 film. The backsides of the silicon substrates were etched in hydrofluoric acid and metallized by evaporating a 100-nm-thick Al layer. Thus, the electrical measurements were carried out on Al/HfO_2/n-Si(100)/Al and Al/HfO_2/SiO_2/p-Si(100)/Al capacitor structures. Capacitance-voltage curves were recorded using a HP 4284A precision LCR-meter. The stair-sweep voltage step was 0.05 V. The period between voltage steps was 0.5 s. The ac voltage applied to the capacitor was 0.05 or 0.005 V while the frequency of the AC signal was either 100 or 500 kHz. The current−voltage curves were measured with a Keithley 2400 Source Meter in the stair sweep voltage mode while the voltage step used was 0.02−0.05 V. All measurements were carried out at room temperature. To check the effect of heat-treatment on dielectric behavior, some HfO_2/SiO_2/p-Si(100) structures grown at 360 °C were annealed first at 450 °C for 30 min in forming gas (95%N_2/5%H_2), following by high-temperature anneal at 850 °C for 4 min under N_2 flow.

3. Results and Discussion.

3.1. Film Growth. In Figure 1, the film growth rate and refractive index are plotted against the substrate temperature. It can be seen that the growth rate increases monotonically with the growth temperature.

(19) Bradley, D. C.; Mehrotra, R. C.; Gaur, D. P. *Metal Alkoxides;* Academic Press: New York, 1978; and references therein.
(20) Bradley, D. C. *Chem. Rev.* **1989**, *89*, 1317
(21) Kukli, K.; Ritala, M.; Leskelä, M. *Chem. Vap. Deposition* **2000**, *6*, 297.
(22) Herrmann, W. A.; Huber, N. W.; Runte, O. *Angew. Chem., Int. Ed. Engl.* **1995**, *34*, 2187.
(23) Williams, P. A.; Roberts, J. L.; Jones, A. C.; Chalker, P. R.; Bickley, J. F.; Steiner, A.; Davies, H. O.; Leedham, T. J. *J. Mater. Chem.* **2002**, *12*, 165.
(24) Williams, P. A.; Roberts, J. L.; Jones, A. C.; Chalker, P. R.; Tobin, N. L.; Bickley, J. F.; Davies, H. O.; Smith, L. M.; Leedham, T. J. *Chem. Vap. Deposition* **2002**, *8*, 163.
(25) Taylor, S.; Williams, P. A.; Roberts, J. L.; Jones, A. C.; Chalker, P. R.; *Electronics Lett.* **2002**, *38*, 1285.
(26) Suntola, T. *Thin Solid Films* **1992**, *216*, 84.
(27) Ylilammi, M.; Ranta-aho, T. *Thin Solid Films* **1993**, *232*, 56.
(28) Jokinen, J.; Haussalo, P.; Keinonen, J.; Ritala, M.; Riihelä, D.; Leskelä, M. *Thin Solid Films* **1996**, *289*, 159.

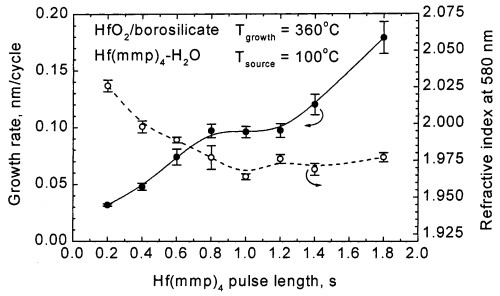

Figure 2. Growth rate and refractive index of HfO_2 films deposited from $Hf(mmp)_4$ and H_2O as functions of Hf precursor pulse length. H_2O pulse lengths and purge periods were 0.5 s. Growth temperatures are indicated by labels. Lines are guides to the eye.

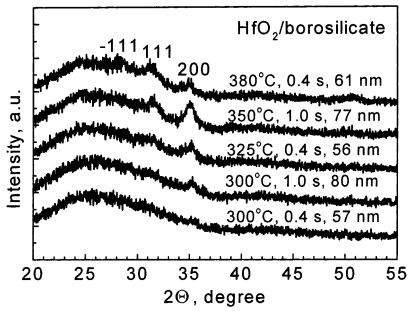

Figure 3. X-ray diffraction patterns of HfO_2 films grown from $Hf(mmp)_4$ and H_2O on glass substrates. Growth temperatures, Hf precursor pulse lengths, and film thicknesses are indicated by labels. H_2O pulse lengths and purge periods were 0.5 s. The reflections are indexed as monoclinic HfO_2.

The increase in the $Hf(mmp)_4$ pulse length from 0.4 to 1.0 s led to the increase in the film thickness deposited during one growth cycle. At the highest temperatures studied, 425 °C, the growth rate exceeded 0.25 Å/cycle. Considering the interatomic distances in HfO_2 (0.2086−0.2197 nm for Hf−O and 0.3547−0.3386 nm for Hf−Hf),[29] it is suggested that at the highest temperatures the average growth rate exceeds one monolayer of hafnium oxide, probably due to the thermal decomposition of the $Hf(mmp)_4$. Fluent increase in the growth rate in the whole temperature range studied indicates that the decomposition of the $Hf(mmp)_4$ likely contributes to the deposition process at all temperatures, becoming gradually more significant toward higher temperatures. Below 300 °C, the precursor reactivities evidently became too low for the film growth with reasonably high rate, and this can probably be attributed to the steric shielding of the Hf center by the methyl groups of the mmp ligand, ($OCMe_2CH_2OMe$).

The refractive index of the films increased from 1.91 and stabilized at 1.97 with the increase in the growth temperature from 300 to 350 °C (Figure 1), while the $Hf(mmp)_4$ pulse length was 0.4 s. In this temperature range, 0.4 s long $Hf(mmp)_4$ pulses resulted in higher refractive index compared to 1.0 s pulse length. In the temperature range of 350−425 °C, no essential differences in the refractive index could be observed. Because the refractive index value is related to the film density, it appears that denser films can be grown using relatively short precursor pulses. Low refractive index in the case of long $Hf(mmp)_4$ pulses may be due to the incomplete hydrolysis of $Hf(mmp)_4$, especially at lower temperatures.

$Hf(mmp)_4$ pulse length was varied at 300, 325, and 360 °C in order to study the effect of the pulse length on the growth rate. Figure 2 demonstrates that at temperatures above 300 °C the adsorption of $Hf(mmp)_4$ cannot be regarded as a self-limiting process. In the rather narrow pulse length range of 0.8−1.2 s the growth rate was still rather stable. It is possible that, due to the considerable size of the precursor molecules, quite long pulses (0.8 s) are required to achieve a stable growth rate. Further, in the case of prolonged precursor pulses (over 1.2 s), thermal decomposition of $Hf(mmp)_4$ will contribute more strongly to the growth rate and the amount of material deposited in one cycle will increase rapidly. HfO_2 may (partially) form also as a result of pyrolysis. Indeed, films could be grown also when only $Hf(mmp)_4$ was pulsed into the reactor without intermediate H_2O pulses at 360 °C. The film grew via pyrolysis with the rate of 0.034±0.005 nm/cycle, which is still three times lower than that in the ALD process with the participation of H_2O. Nevertheless, the refractive index of the resulting films was 2.000±0.005 indicating that at relatively high temperatures and with long pulses quite dense films may be grown even without hydrolysis steps.

3.2. Film Structure and Composition. Figure 3 demonstrates X-ray diffraction patterns of the HfO_2 films deposited at different temperatures on borosilicate glass substrates. Obviously, the crystal growth on the amorphous substrate is rather weak. It can still be seen that the films grown at higher temperatures become more crystallized. The crystal growth could also be slightly intensified by applying longer $Hf(mmp)_4$ pulses. The reflections can be assigned as belonging to the monoclinic polymorph of HfO_2[30], although the width of the peak at 35.4° does not allow one to distinguish between monoclinic and metastable phases possibly existing in the film. A peak characteristic to the tetragonal or orthorhombic phase, which should appear also in ALD films at 30.03°,[10,11,31] was not detected in this study. Therefore, the films may be considered to consist dominantly of the monoclinic polymorph. No qualitative differences between the phase contents of the films grown on glass and silicon substrates were observed. Nonetheless, in the films grown on Si, all the reflections of the monoclinic phase were considerably more intense compared to those of the films on glass substrates. The increase in the water dosing[32] did not cause substantial differences in the films crystallinity (Figure 4). Judged on the basis of the width of reflection peaks, one can conclude that the crystallite sizes are really low and nanocrystalline films were thus formed during the growth process.

According to TOF-ERDA, the hafnium and oxygen concentrations were 24−30 (±2) and 53−64 (±2) at. %, respectively, in the films grown in the temperature range of 300−400 °C (Table 1). So the oxygen-to-hafnium ratio ranged from 2.2 to 2.0 in these samples.

(29) Wang, Li, H. P.; Stevens, R. *J. Mater. Sci.* **1992**, *27*, 5397.

(30) International Centre for Diffraction Data, (ICDD), Newtown Square, PA, Powder Diffraction File, Card 431017.

(31) Kukli, K.; Ritala, M.; Sajavaara, T.; Keinonen, J.; Leskelä, M. *Thin Solid Films* **2002**, *416*, 72.

(32) Matero, R.; Rahtu, A.; Ritala, M.; Leskelä, M.; Sajavaara, T. *Thin Solid Films* **2000**, *368*, 1.

Table 1. Elemental Composition of HfO_2 Films Grown on Silicon, Measured by TOF-ERDA

T_{growth}, °C	state	t_1, s	O, at.%	Hf, at.%	H, at.%	C, at.%	Zr, at.%
300	as-deposited	0.4	54 ± 3	24 ± 2	14 ± 3	6 ± 2	0.4 ± 0.1
300	as-deposited	1.0	53 ± 2	24 ± 2	18 ± 4	4 ± 1	0.4 ± 0.1
360	as-deposited	0.4	56 ± 2	26 ± 2	12 ± 2	6 ± 2	0.2 ± 0.1
360	annealed	0.4	64 ± 2	30 ± 2	2.2 ± 0.5	2.2 ± 0.5	0.5 ± 0.1
400	as-deposited	0.4	56 ± 3	26 ± 2	12 ± 2	6 ± 2	0.4 ± 0.1
425	as-deposited	1.0	59 ± 2	30 ± 2	7 ± 1	2.6 ± 0.5	0.3 ± 0.1

[a] t_1 is the length of hafnium precursor pulse.

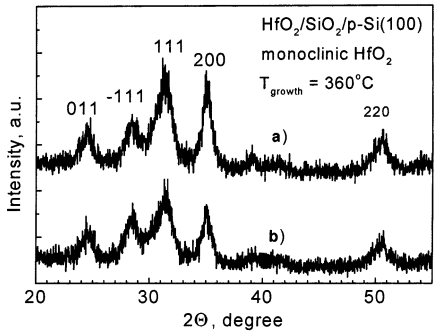

Figure 4. X-ray diffraction patterns of selected HfO_2 films grown from $Hf(mmp)_4$ on silicon substrates. Growth temperatures are indicated by labels. The reflections are indexed as monoclinic HfO_2. H_2O pulse lengths and purge periods were 0.5 s. The H_2O consumption during the growth was 8×10^{-6} g/s (a) or 2×10^{-4} g/s (b).

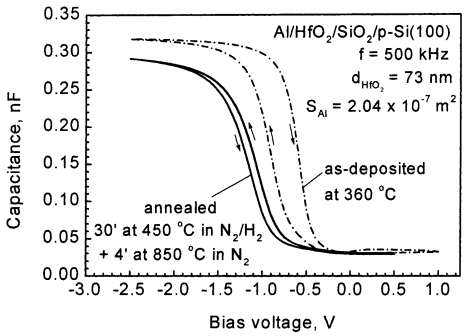

Figure 5. Capacitance−voltage and dissipation curves measured for $Al/HfO_2/SiO_2$/p-Si(100) with capacitor at a.c. signal frequency of 500 kHz.

Thus, the films tended to contain some excess oxygen, which may arise from the excess water or hydroxyl groups in the films and, possibly, from the unreacted ligands. This is supported also by the rather high contents of residues in the films. Impurities create defect levels in oxide band gap both in film bulk and at oxide/silicon interface, affect phase transformations, and generally lower the density of the oxide material. On the other hand, it is not clear how high initial impurity levels are actually tolerable in the CMOS devices. Impurities may be annealed out by postdeposition heat-treatment. The eventual purity of the material may still depend on the initial impurity content as well as the duration and temperature of annealing. Therefore, it is important to know the initial elemental composition and impurity contents.

The carbon and hydrogen levels remain in the range of 2.6−6.0 and 2.2−18 at. %, respectively. The lowest contamination levels were measured in the films grown at the highest temperature, 425 °C, and in the annealed samples. Generally, the contaminants were distributed homogeneously throughout the films' thickness. In some samples, hydrogen and carbon peaks were detected at the film surface, likely coming from water and organic contaminants while stored in ambient air. Zirconium, the common impurity in hafnium compounds, was also found in all of the HfO_2 films but in concentrations not exceeding 0.2−0.5 at. %.

3.3. Dielectric Properties. Figure 5 demonstrates capacitance−voltage (C−V) curves for the $Al/HfO_2/SiO_2$/p-Si(100) MOS structure with HfO_2 films deposited at 360 °C. It can be seen that the curves demonstrate features characteristic of well-insulating dielectric material with accumulation region at negative biases, depletion and inversion at positive biases.[33,34] The total capacitance of the MOS structure is a series combination of the oxide capacitance and the semiconductor depletion layer capacitance. When the semiconductor next to the oxide is depleted from charge carriers, the capacitance of the depletion layer is equal to ϵ_{Si}/w, where ϵ_{Si} is the semiconductor permittivity and w is the width of the depletion layer. The stronger the depletion, the broader the depletion layer and smaller the layer capacitance, causing the decrease in total capacitance. The depletion layer broadens until an inversion layer forms at the interface from minority carriers at strong positive bias, screening the field in the semiconductor, and resulting in the minimum capacitance in C−V curves. On the other hand, at negative bias voltages, there occurs an accumulation of majority carriers at the semiconductor/oxide interface and there is no depletion region. As a result, the measured maximum capacitance is very close to the oxide (HfO_2) capacitance. In the case of n-type substrates (Figure 6) the polarities are changed, depletion occurs at negative biases, and the general shape of C−V curves is correspondingly mirrored. To calculate the effective permittivity of the insulating material, the simple parallel plate capacitor model can be applied, where the measured capacitance is taken from the accumulation region of C−V curves.

It is noteworthy that the C−V curves measured on as-deposited films demonstrated clockwise hysteresis when swept from positive to negative bias forward, and from negative to positive bias backward. This can be attributed to the mobile charge existing in the films,[33] while for large positive bias ions (such as H^+) could drift to the silicon−oxide interface, giving a negative capacitance−voltage shift. For strong negative bias, this charge is attracted to the gate electrode−oxide interface. In addition, the oxide layer should contain considerable density of electron traps because the flat-band voltage of the C−V curves of as-deposited films is generally

(33) Schröder, D. K. *Semiconductor Material and Device Characterization*, 2nd ed.; Wiley and Sons: New York, 1998; p 350.

(34) Sze, S. M. *Physics of Semiconductor Devices*, 2nd ed.; Wiley: New York, 1998; p 350.

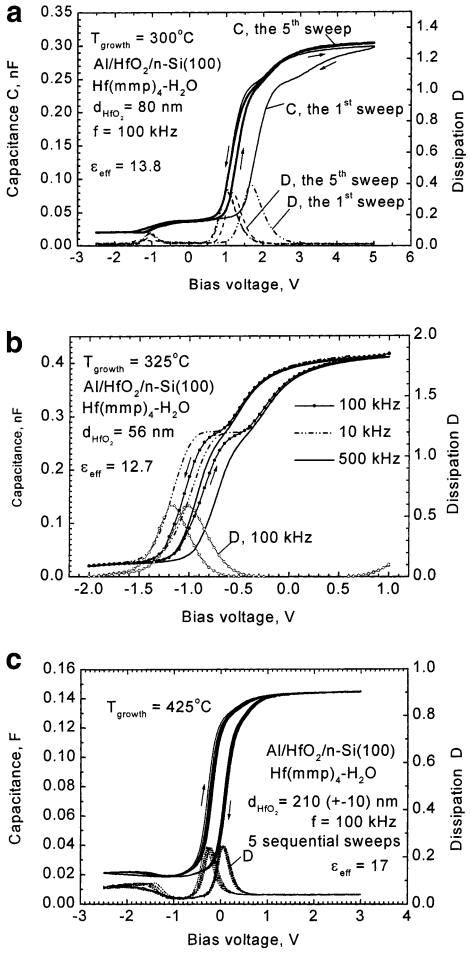

Figure 6. Capacitance−voltage and dissipation curves measured for Al/HfO_2/n-Si(100) capacitors with HfO layers as-deposited at 300 °C (a), 325 °C (b), and 425 °C (c).

shifted toward positive bias by about 0.5 V, whereas the flat-band voltage of ideal MOS structures with Al and p-Si electrodes and perfect oxide/semiconductor interface should be at around −0.9 to −1.0 V.[34] The capacitance−voltage behavior obviously improves after the annealing procedure, because the hysteresis width decreases and the loop changes its direction. The accompanying decrease in accumulation capacitance may be due to the development of an interface SiO_2 layer but also due to the decreasing contribution from the interfacial polarization.

The C−V behavior was also examined for the Al/HfO_2/n-Si(100) structures with the HfO_2 films grown at three different temperatures (Figure 6). The characteristic features of the C−V curves were different at each deposition temperature. At the lowest temperature, 300 °C, the C−V curves were rather unstable. The hysteresis widths of the C−V curves repeatedly measured on the same capacitor were decreasing and the hysteresis loop changed its direction as well (Figure 6a). At higher temperatures, 325 °C, the hysteresis (width) was more stable. In C−V curves, a shoulder-like feature appeared in the inversion region during both forward and backward sweeps (Figure 6b). This shoulder has earlier appeared in the sputtered HfO_2 films[35] as well as in the

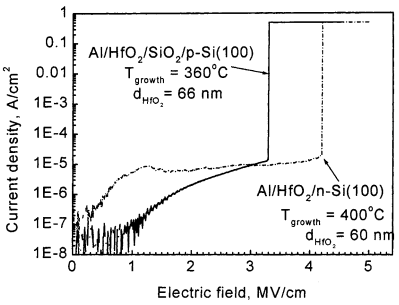

Figure 7. Leakage current density versus electric field curves for selected MOS capacitors. Majority carriers in Si substrate were injected into oxide.

ALD films.[31] The shoulder may arise from the charge released and/or trapped at deep interface traps. Indeed, a pronounced feature in the C−V curves was the dependence of the shoulder on the measurement frequency, while the shoulder almost disappeared at the highest frequency used, 500 kHz. Thus, it is likely that the traps are deep enough to require relatively long response time. At the highest temperature studied, 425 °C, the C−V curves were most stable without shoulder-like features and resisting repetitive sweeping without considerable change in hysteresis width and direction (Figure 6c). The effective permittivities of the dielectric layer in these capacitors, calculated from the accumulation capacitance considering simple parallel-plate capacitor structure, were 13.8, 12.7, and 17.0 at growth temperatures 300, 325, and 425 °C, rather irrespectively to the measurement frequency.

The current−voltage behavior was examined for some abovementioned capacitors. The leakage current density versus electric field curves demonstrated that the current density remained below 1×10^{-5} A/cm^2 until the dielectric breakdown (Figure 7). The breakdown occurred typically at electric field values exceeding 3 MV/cm. Annealing resulted in a considerable reduction of the breakdown field down to 1.0−1.5 MV/cm (not shown), apparently due to the crystallization and the related development of leaky grain boundaries.

Finally, it should be noted that this work proves that hafnium oxide films can be grown by atomic layer deposition technique using Hf(OCMe$_2$CH$_2$OMe)$_4$ and H_2O as precursors. Although the impurity levels are high, the basic stoichiometry of the oxide corresponds to that of dioxide and the films behave as well-defined dielectric layers. The adsorption process of the hafnium precursor is not self-limiting. The self-limitation can be expected only at relatively low temperatures below 325 °C, still not enabling the growth of the material of maximum density. To compare these films adequately with films obtained using other processes and clarify their suitability for certain applications such as high-permittivity gate oxides, the effect of the film thickness and annealing conditions on the structure, purity, and dielectric performance has to be studied separately.

3. Summary

HfO_2 films consisting of the monoclinic phase were grown by atomic layer deposition using Hf(mmp)$_4$ and H_2O as metal and oxygen precursors in the temperature range of 275−425 °C on borosilicate glass and Si(100) substrates. The adsorption of Hf(mmp)$_4$ was not per-

(35) Callegari, A.; Cartier, E.; Gribelyuk, M.; Okorn-Schmidt, H.-F.; Zabel, T. *J. Appl. Phys.* **2001**, 90, 6466.

fectly saturating but the growth rate was enhanced by the thermal decomposition of $Hf(mmp)_4$. The films deposited possessed O/Hf ratio in the range of 2.0−2.2. The refractive index of the films varied between 1.8 and 2.0. The effective permittivities of the dielectrics in Al/HfO_2/Si structures varied between 12 and 17. The capacitance−voltage curves demonstrated clockwise, 1−2 V wide, hysteresis indicating the likely contribution of positively charged ions in the conduction and polarization process.

Acknowledgment. The study was partially supported by Academy of Finland (Projects 51989, 43329, and 44215).

CM021328P